

# The Orbiting Wide-angle Light-collectors (OWL) Mission for Charged-Particle Astronomy

J.W. Mitchell\*, J.F. Krizmanic<sup>\*,1</sup>, F.W. Stecker\*, R.E. Streitmatter\* for the OWL Collaboration

\*NASA/GSFC, Greenbelt, MD 20771, USA

**Abstract.** The OWL mission is designed to advance the field of charged-particle astronomy with high-statistics measurements of ultra-high-energy cosmic rays (UHECR) using the Earth's atmosphere as a vast particle calorimeter. OWL employs two large formation-flying telescopes in near-equatorial orbits to stereoscopically image the near-UV air fluorescence from UHECR-induced particle cascades. Stereo allows precise event reconstruction that is nearly independent of the inclination of the particle track and tolerant of atmospheric conditions. HiRes and Auger have confirmed the GZK cutoff above  $\sim 6 \cdot 10^{19}$  eV, implying an astrophysical origin for the majority of UHECR. Sources of particles above the GZK threshold must lie within about 100 Mpc. Under standard estimates of extragalactic magnetic field strength, the paths of these UHECR will be deflected by only a few degrees, so individual sources may be identified and characterized. Auger South, Telescope Array, and, possibly, Auger North will open the field of charged-particle astronomy. However, much larger exposures will be required to identify individual sources and measure spectra. A five-year OWL mission would deliver  $\sim 10^6$  km<sup>2</sup> sr yr of exposure with full aperture reached at  $\sim 10^{19}$  eV. OWL can also measure horizontal or upward-moving showers from UHE neutrino events.

**Keywords:** OWL Mission, UHECR, GZK, air fluorescence, charged-particle astronomy

## I. INTRODUCTION

The OWL (Orbiting Wide-angle Light-collectors) mission [1] is designed to answer one of the outstanding mysteries in particle astrophysics, the source of ultra-high-energy cosmic rays (UHECR) [2,3] that have been detected to energies  $> 10^{20}$  eV [3-6]. Recent confirmation [7,8] of the Greisen-Zatsepin-Kuzmin (GZK) suppression [9,10] above  $\sim 6 \cdot 10^{19}$  eV suggests that acceleration in astrophysical engines, such as active galactic nuclei (AGN) or  $\gamma$ -ray bursts, can power the UHECR spectrum. Explanations requiring new physics, such as the decay of topological defects, are disfavored by these data. This opens the possibility of charged particle astronomy as a new window on the high-energy Universe. UHECR above the GZK cutoff (super-GZK) must come from sources within  $\sim 100$  Mpc and are

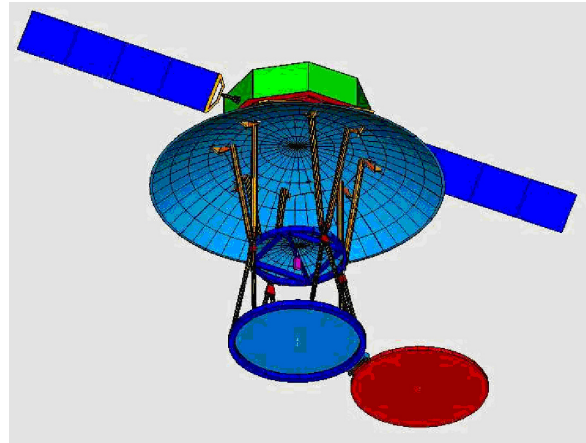


Fig. 1: Fully deployed OWL instrument with light shield removed for clarity.

estimated to deflect at most a few degrees traversing extragalactic magnetic fields. Ultra-high-energy neutrinos (UHE $\nu$ ) from GZK interactions or directly from sources may provide additional information on the acceleration engines. The UHECR flux is  $\sim 1$  km<sup>-2</sup> century<sup>-1</sup>, and exposures of  $\sim 10^6$  km<sup>2</sup> sr yr are needed to identify individual sources and measure their spectra.

OWL determines the energy and arrival directions of UHECR using the Earth's atmosphere as an immense particle detector by measuring near-UV fluorescence from airshowers. Energy resolution is  $\sim 15\%$  and angular resolution is  $< 1^\circ$ . Initially funded by NASA as a "New Mission Concept" in 1996, OWL has been the subject of an extensive development effort, including 2002 studies in the GSFC Instrument Synthesis and Analysis Laboratory (ISAL) and Integrated Mission Design Center (IMDC). OWL uses two large co-orbiting telescopes, one of which is shown in Figure 1, to give detailed stereo images of the spatial and temporal evolution of UHECR showers. Stereo enables precise event reconstruction that is nearly independent of the inclination of the particle track and of atmospheric conditions. OWL is also capable of monocular operation, which increases reliability or could be employed to increase the instantaneous aperture. In stereo mode, OWL has exceptional sensitivity for UHE $\nu$  detection by fully reconstructing near-horizontal or upward-moving showers. The baseline OWL telescopes can fly as a dual manifest on a single Evolved Expendable Launch Vehicle (EELV). A five-year OWL mission would deliver  $\sim 10^6$  km<sup>2</sup> sr yr of exposure with full aperture reached by  $\sim 1.4 \cdot 10^{19}$  eV at 600 km altitude and  $\sim 4 \cdot 10^{19}$  eV at 1000 km.

<sup>1</sup>Also Universities Space Research Association, Columbia, MD.

### A. Ultra-High-Energy Cosmic Rays

The first detection of a  $10^{20}$  event was reported in 1963 [2]. At energies above a few  $10^{19}$  eV, UHECR are expected to interact with the cosmic microwave background (CMB), resulting in the GZK suppression of flux from distant sources. Protons lose energy by pion photoproduction and composite nuclei suffer photodisintegration. Events well above  $10^{20}$  eV were reported by Fly's Eye [4] and AGASA [5]. The GZK cutoff was not evident, however, leading to suggestions that UHECR might originate in exotic local processes. In 2008, HiRes [7] reported observation of the GZK cutoff from  $3 \times 10^3$  km<sup>2</sup> sr yr of exposure, Figure 2a, indicating the probable origin of UHECR in astrophysical objects, and opening the possibility of identifying sources in the nearby extragalactic universe using the arrival directions of super-GZK cosmic rays. Auger [8] confirmed this from  $7 \times 10^3$  km<sup>2</sup> sr yr, Figure 2b. Particle sources must lie within  $\sim 150$  Mpc at  $4 \times 10^{19}$  eV, falling to  $< 10$  Mpc at  $10^{20}$  eV. The GZK radius also depends on species. Light composite nuclei photodisintegrate in a short distance while protons and iron may come from greater distances. In any case, super-GZK particles must come from sources within a limited distance and are expected to be deflected little by extragalactic magnetic fields. Thus, if UHECR sources follow the distribution of luminous matter, then the arrival directions of super-GZK particles should exhibit an anisotropic distribution and perhaps a correlation with sources.

Potential accelerators to super-GZK energies range from neutron stars, AGN, and  $\gamma$ -ray bursts to cluster shocks. Significant anisotropy was first reported by Auger in 2007 as a correlation in the arrival directions of 27 events above  $5.7 \times 10^{19}$  eV with AGN [11]. Analysis of an independent dataset confirmed anisotropy at a confidence level  $> 99\%$ . HiRes [12], however, examined their 13 highest energy events and found the distribution to be consistent with isotropy at 97% probability. The latest reports from Auger [13] indicate a weaker correlation with AGN, but still good correlation with the matter distribution. With the small number of events, it is not clear what these results may indicate about the sources or their distribution. The Auger anisotropy results indicate a correlation with luminous matter. However, the HiRes results do not.

Identifying and characterizing the cosmic accelerators will require enough exposure to clearly show correlations, or lack thereof, and ideally to measure the spectra of individual sources. Spectral measurements will probe source density and evolution, and may test fundamental physics. Theories of the nature of space-time approaching the Planck scale can admit or imply violations of Lorentz invariance, which may modify the GZK effect above  $10^{20}$  eV [14], leading to a recovery of the spectrum. Each year, existing ground detectors will provide  $\sim 9 \times 10^3$  km<sup>2</sup> sr yr (Auger South  $7 \times 10^3$  km<sup>2</sup> sr yr [6], Telescope Array  $\sim 1.5 \times 10^3$  km<sup>2</sup> sr yr [15]), but

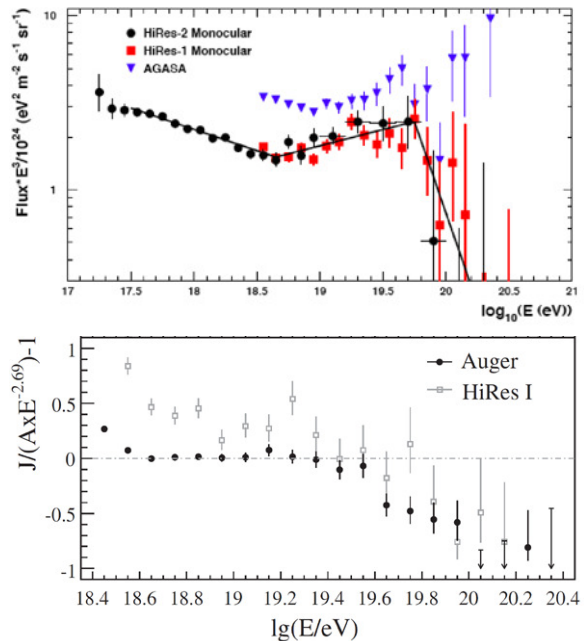


Fig. 2: (a) HiRes and AGASA UHECR flux  $\times E^3$  [7]; (b) Deviation of Auger and HiRes flux from  $E^{-2.69}$  [8].

fewer than 500 super-GZK events are expected by 2020. By comparison, a 5-year OWL mission would measure over 5,000 super-GZK events.

### B. Ultra-High-Energy Neutrinos

$\text{UHE}\nu$  are expected from GZK interactions and from suggested UHECR sources, but with an uncertain flux depending on UHECR spectra and source evolution. Neutrinos are not deflected by magnetic fields and, therefore, can probe sources beyond the GZK horizon. Cross-sections are small, and current UHE observatories may detect a few  $\text{UHE}\nu$  per year above  $\sim 10^{18}$  eV. OWL will have enhanced sensitivity for  $\text{UHE}\nu$  at higher energies by detecting near-horizontal showers from interactions in the huge atmospheric target and upward-moving showers from interactions in the Earth.

## II. OWL INSTRUMENT AND MISSION

OWL uses the Earth's atmosphere as a huge imaging calorimeter to accurately determine the energy, arrival direction, and interaction characteristics of UHECR. Excitation of atmospheric nitrogen molecules by shower particles produces a UV luminous disk, a few meters thick and  $\sim 100$  m wide, that moves through the atmosphere at the speed of light. OWL uses a fast, highly pixelized camera (eye) to resolve shower spatial and temporal development. The UV emission, at 300-400 nm, is isotropic. A single camera can view a large volume of atmosphere, limited only by atmospheric absorption and obscuration. Both monocular and stereo techniques are possible. In monocular operation, an individual camera images the projection of the shower onto a plane normal to the viewing direction. Distance from the camera must be resolved using other information. Differential arrival times of photons along the shower

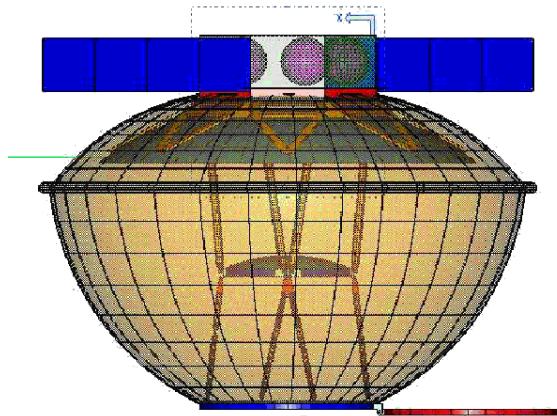


Fig. 3: Fully deployed OWL satellite. Light shield is translucent to show interior.

track can resolve the angle of the shower relative to the viewing plane. Resolving absolute distance by timing, however, requires measuring the pixel crossing time to an accuracy that is unlikely to be practical in a flight instrument. Viewed from space, the Cherenkov spot of tracks that intersect the ground can establish distance, but this greatly reduces the aperture since tracks with shallow inclination may leave the viewing area. Stereo observation completely resolves all three spatial dimensions and confers the crucial advantages that atmospheric light absorption or scattering can be corrected and tracks that do not intersect the ground can be reconstructed. The HiRes results viewing the same shower in both modes clearly demonstrate the superiority of stereo. The fast timing incorporated in OWL for mono operation provides supplementary track information in stereo.

OWL employs a pair of formation-flying spacecraft in low-inclination, medium-altitude orbits. The instruments view  $>5 \cdot 10^5 \text{ km}^2$  of common detector area for an instantaneous aperture of  $2 \cdot 10^6 \text{ km}^2 \text{ sr}$ . The satellites are launched as a dual manifest on an EELV into 1000 km circular orbits with a nominal inclinations of  $10^\circ$ . The satellites initially fly with a separation of 10-20 km for  $\sim 3$  months to search for neutrinos that pass through the Earth and initiate upward-going showers. The spacecraft then separate to 600 km for  $\sim 2.5$  years to measure the high-energy end of the UHECR spectrum. For the rest of the mission, altitude is decreased to 600 km with 500 km separation, to reduce the detection threshold and measure lower energies. The orbits were chosen based on a trade among the collecting power, the angular FOV of the optical system, and the energy threshold of the instrument. During the 1000 km viewing period, the leading instrument is pitched back 14 degrees from nadir, and the trailing instrument is similarly pitched forward 14 degrees. Each instrument is completely shuttered whenever it might be exposed to direct or reflected sunlight or significant moonlight. The OWL baseline instrument and mission can be realized using current technology and are not dependent on new developments.

The instruments function completely independently and do not require space-to-space communication. Data are combined on the ground using GPS time stamps. Event triggers use hierarchical hardware and software algorithms to suppress background and localize shower tracks on the focal plane. A hardware trigger designed for very high efficiency and minimal dead time initiates acquisition in a limited region of the focal plane around the point where the trigger was generated. More selective hardware and computed triggers refine the viewed region and select events, limiting the data volume without introducing significant efficiency systematics except near threshold. All data acquired can be telemetered and no on-board reduction is required. After event location and crude track determination, a series of laser shots are automatically taken along the track by each instrument to determine local atmospheric conditions. In addition, a random scan of the FOV is made at approximately one laser shot per second to characterize the average cloud obscuration. This is complemented by data obtained from IR-imaging satellites.

#### A. Spacecraft

OWL requirements are relatively modest, and the three-axis stabilized spacecraft is entirely conventional. The instrument mass is 1800 kg, and the spacecraft is 1440 kg, making one satellite 3240 kg at launch. Required pointing accuracy is only about  $2^\circ$  with a knowledge of  $0.01^\circ$ . The instrument uses 600 W, and the spacecraft 430 W. The data rate averages 150 kbps, dominated by calibration and atmospheric monitoring. Telemetry uses S-band, averaging 192 kbps during the active viewing period and 12 kbps otherwise. Mission operations are largely autonomous and consist mainly of health and well-being monitoring except during early operations and orbit changes.

#### B. Optical System

The OWL optical system is a low-resolution imager, or light bucket, with more similarities to a microwave system than to a precision optical telescope. Showers are at most several tens of kilometers in length, and the natural measurement scale is about 1 kilometer. The corresponding optical angular resolution depends on the orbit altitude. At 1000 km an angular resolution of only 1 milliradian is needed, over 3 orders of magnitude larger than the diffraction limit, and only 1.7 milliradian at 600 km. The baseline is an f/1 Schmidt camera with a  $45^\circ$  full FOV and a 3.0 m diameter corrector. The deployable primary mirror is 7 m in diameter. The focal plane area is  $4 \text{ m}^2$  with  $\sim 5 \cdot 10^5$  pixels. An absorption filter with a tailored bandpass, 330 to 400 nm, suppresses background. Including obscuration by the focal plane, the effective aperture is  $3.4 \text{ m}^2$ . The primary is a lightweight composite with a central octagonal section and eight petals. The satellites launch with the primary petals folded upward, the corrector collapsed on the focal plane, some shield material in a storage volume, and the

shutter closed. After deployment and activation of the focal plane and the instrument electronics systems, the petals are aligned using actuators to focus a point light source located at the center of curvature of the primary.

The entire optical system is covered by an inflatable light and micrometeoroid shield and is closed out by a redundant shutter system. The shield incorporates an inflatable support ring and strengthening/shaping ribs that can be rigidized after inflation. The full instrument/spacecraft with deployed shield is shown in Figure 3. A UV laser for atmospheric characterization is located at the back of the focal plane and fires through the center of the corrector to a small steering mirror system. Laser light reflected by clouds is detected and measured using the OWL focal plane.

### C. Focal Plane and Electronics

The focal plane detects light in  $0.1 \mu\text{s}$  intervals to track the shower as it crosses each pixel FOV ( $3.3 \mu\text{s}$  for a shower perpendicular to the viewing direction to cross 1 km). Sub-pixel timing improves reconstruction systematics and angular resolution, and supports monocular operation. Signal-to-noise ratio (S/N) limits the lowest signal (lowest particle energy) that can be measured, and single photoelectron detection dictates the use of multi-anode vacuum photomultipliers or silicon photomultipliers. On each pixel, a switched capacitor array (SCA), with 3000 cells switching at 10 MHz, acts as an analog ring buffer.

For triggering, signals are integrated for  $3.3 \mu\text{s}$  to maximize S/N. The trigger logic examines the spatial and temporal signal development for typically 3 pixels and integration times around each pixel that exceeds a threshold that adapts automatically for background light. The trigger fires at about 35 Hz and engages less than 3% of the focal plane each time. Thus, the effective trigger rate in any region is about 1 Hz. Following a trigger, a look-up table identifies the viewed region of pixels. The  $300 \mu\text{s}$  SCA analog storage spans 90 pixel crossing times. Unless a higher-level hardware trigger stops the process, the SCAs in the viewed region are halted after  $200 \mu\text{s}$  and read out, recording 30 pixel crossing times before the trigger and 60 after, so the trigger can be generated at any point from the start of a shower to its peak. Events are selected within 2 sec of triggers, and fast track determination enables the LIDAR laser to slew and scan. A separate fast trigger detects upward-going neutrino events when the satellites are separated less than the width of the Cherenkov light pool.

### D. Atmosphere and Cloud Monitoring

Events observed by OWL will occur in an enormous footprint (size of the state of Utah) moving across the globe at a speed of 7 km/sec. This will include variable amounts of cloud with altitudes from sea level to 15 km and variable boundary layer aerosols. Consistency between the stereo views of an event provides a powerful tool for understanding scattering through intervening

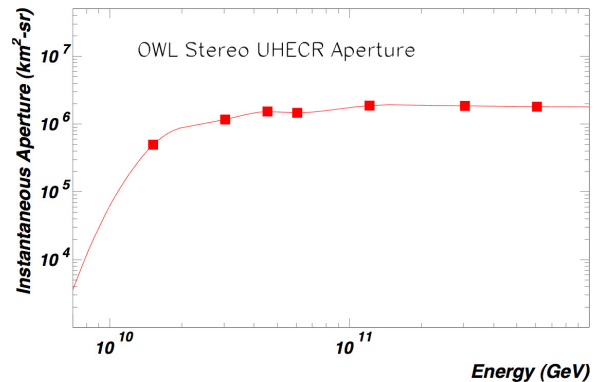


Fig. 4: Owl stereo aperture at 1000 km vs. energy

high clouds or aerosol layers. OWL also uses a steerable UV laser and the OWL telescope as a LIDAR for real-time atmosphere characterization and for a sparse scan of the full FOV to determine the average aperture. The OWL instruments conduct independent laser scans over the region of an event, and the failure of one laser would not result in a significant loss of capability.

### E. Viewing Efficiency

Each OWL eye must remain shuttered until the viewed Earth has entered full darkness, resulting in a duty factor of 14.4%. Man-made light, oceanic effects, lightning, and clouds [16] give an overall efficiency of 11.5%. Adaptive trigger thresholds improve this value by accommodating light sources that vary slowly compared to the pixel crossing time, such as lightning and man-made light. OWL measurement efficiency has been examined using a detailed Monte Carlo technique with realistic shower generation, atmospheric light propagation, and instrument response. Position and orientation of the shower track, particle energy, trigger selectivity, and event reconstruction have been included. The energy-dependent efficiency is lowest near the detection threshold and rises to nearly 100% for higher energies, illustrated in Figure 4 showing the OWL UHECR aperture at 1000 km altitude vs. energy for stereo events. The conservative continuous aperture is  $2.3 \times 10^5 \text{ km}^2 \text{ sr}$ . For each year of operation, OWL has 230 times the aperture of HiRes and 33 times the aperture of the Auger South surface detectors (330 times the Auger hybrid aperture).

### REFERENCES

- [1] owl.gsfc.nasa.gov/
- [2] J. Linsley 1963, Phys. Rev. Lett. 10, 146
- [3] A. Olinto *et al.* 2009, arXiv:0903.0205
- [4] www.cosmic-ray.org/
- [5] www-akeno.icrr.u-tokyo.ac.jp/AGASA/
- [6] www.auger.org/
- [7] R.U. Abbasi *et al.* 2008, Phys. Rev. Lett., 100, 101101
- [8] J. Abraham *et al.* 2008, Phys. Rev. Lett., 101, 061101
- [9] K. Greisen 1966, Phys. Rev. Lett., 16, 748
- [10] G.T. Zatsepin and V.A. Kuzmin 1966, Zh. Eksp. Teor. Fiz. 4, 114; JETP Lett. 4, 7
- [11] J. Abraham *et al.* 2008, Astropart. Phys. 29, 188
- [12] R.U. Abbasi *et al.* 2008, Astropart. Phys. 30, 175
- [13] D. Zavrtnik for P. Auger Collab. 2009, RICAP'09 (Rome)
- [14] S.T. Scully and F.W. Stecker 2009, Astropart. Phys. 31, 220
- [15] www.telescopearray.org/
- [16] P. Sokolsky and J. Krizmanic 2004, Astropart. Phys. 20, 391